LIMNOLOGY and OCEANOGRAPHY

ASLO

Limnol. Oceanogr. 9999, 2024, 1–16

doi: 10.1002/lno.12605

Multi-omics analyses reveal the signatures of metabolite transfers across trophic levels in a high-CO_2 ocean

Mengcheng Ye,[1] Jiale Zhang,[1] Mengting Xiao,[1] Jiali Huang,[1] Yunyue Zhou,[1] John Beardall,[2] John A. Raven,[3,4,5,†] Guang Gao,[6] Xiao Liang,[1] Fenghuang Wu,[1] Baoyi Peng,[1] Leyao Xu,[1] Yucong Lu,[1] Shiman Liang,[1] Yipeng Wang,[1] Hao Zhang,[1] Jingyao Li,[1] Ling Cheng,[7] Zuoxi Ruan,[8] Jianrong Xia,[1] Peng Jin[1*]

[1]School of Environmental Science and Engineering, Guangzhou University, Guangzhou, China
[2]School of Biological Sciences, Monash University, Clayton, Victoria, Australia
[3]Division of Plant Science, University of Dundee at the James Hutton Institute, Invergowrie, Dundee, UK
[4]School of Biology, University of Western Australia, Crawley, Western Australia, Australia
[5]Climate Change Cluster, University of Technology, Sydney, Ultimo, New South Wales, Australia
[6]State Key Laboratory of Marine Environmental Science, College of Ocean and Earth Sciences, Xiamen University, Xiamen, China
[7]Gene Denovo Biotechnology Co., Guangzhou, China
[8]STU-UNIVPM Joint Algal Research Center, Marine Biology Institute, Shantou University, Shantou, Guangdong, China

Abstract

Although the diverse impacts of elevated dissolved CO_2 and warming on organisms within various trophic levels in marine food webs are well documented, we have yet to explore the biological links across different levels of biological organization from primary producers to secondary producers on an evolutionary time scale in a high-CO_2 ocean. Here, we cultured a model marine diatom *Phaeodactylum tricornutum* (primary producer) in predicted future high-CO_2 and/or warming conditions for ~ 1250 d with an experimental evolution approach and then fed them to the clam *Coelomactra antiquata* (secondary producer). We present an in-depth multi-omics analysis along the methylome (primary producer)–transcriptome (primary producer)–metabolome (primary producer)–metabolome (secondary producer) continuum. Our results showed that the downregulated terpenoid backbone biosynthesis in the methylome and transcriptome lead to decreased pyruvate levels and upregulation of some pathways (such as phenylalanine metabolism) in the metabolome of the primary producer in the long-term warming conditions. These changes in metabolomic profile in the primary producer were then transferred to the secondary producer, resulting in changes in abundance of some metabolites, such as decreases in pyruvate, and in pyruvaldhyde (also known as methylglyoxal), and increases in 2-hydroxylamino-4,6-dinitrotoluene. Our study provides a new insight into the molecular mechanisms underlying the trophic transfer from primary to secondary producers in a future high-CO_2 ocean and may provide more accurate projections of marine ecosystem services and functions over the next century.

Increasing dissolved CO_2 and rising sea surface temperature (ocean warming) are recognized as two major anthropogenic disturbances in the modern ocean (IPCC 2021). There is an extensive literature that demonstrates the diverse impacts of elevated CO_2 and ocean warming on organisms at various trophic levels in marine food webs (Clark et al. 2020; Nagelkerken et al. 2020, Taucher et al. 2022). Furthermore, a limited but growing body of research highlights the potential transfer of biochemical changes (such as fatty acids, phenolic compounds, amino acids) induced by elevated CO_2 to higher trophic levels, subsequently influencing their performance and disrupting marine food webs (Rossoll et al. 2012; Jin et al. 2015; Riebesell et al. 2018; Sswat et al. 2018). Understanding these effects within food chains holds the key for more accurate projections of the cumulative impacts of marine environmental changes on communities and ecosystems (Hurd et al. 2018).

*Correspondence: pengjin@gzhu.edu.cn

Additional Supporting Information may be found in the online version of this article.

Author Contribution Statement: PJ conceived and designed the study. PJ, MY, JZ, MX, JH, YZ, XL, FW, BP, LX, YL, SL, YW, HZ, and JL acquired the data. PJ, JB, JAR, GG, LC, ZR, MY, JZ, and JAR analyzed and interpreted the data. PJ drafted the manuscript. JB and JAR commented on drafts and contributed to the editing of the manuscript.
MY, JZ, MX, and JH contributed equally to this study.
[†]Deceased.

Marine microalgae, which lie at the base of most marine food webs, exhibit high capacity for rapid evolutionary responses to marine environmental changes (Schlüter et al. 2014; Listmann et al. 2016). This is attributed to their short generation time, high population densities, and standing genetic variability (Reusch and Boyd 2013; Collins et al. 2020). It was shown that the adaptation of the coccolithophorid *Emiliania huxleyi* to ocean warming occurred independently to high CO_2, and the magnitude of the growth adaptation to warming was roughly three times larger than the adaptation to high CO_2, suggesting that ocean warming is more likely to be the main driver for the evolution of phytoplankton rather than high CO_2 (Schlüter et al. 2014). It was also reported that the marine diatom species *Phaeodactylum tricornutum* displayed substantial genetic diversity losses and genetic differentiation following a 2-yr adaptation to elevated CO_2 and/or warming conditions (Jin et al. 2022*b*). Furthermore, it was also shown that DNA methylation acted cooperatively with gene transcription, resulting in changes in phenotypic traits such as photosynthesis and respiration, facilitating adaptation (Wan et al. 2023). This multi-omics approach established a link across different levels of biological organization. Building upon these insights, we postulate that alterations in the methylome and transcriptome modulate the content and composition of phytoplankton metabolites, thereby influencing food quality and subsequently impacting the metabolite profiles of consumers feeding on them. However, the manner in which this connection extends across trophic levels, such as from primary producers to secondary producers, remains unexplored. To address this knowledge gap, we here present an in-depth multi-omics analysis along the methylome (primary producer)–transcriptome (primary producer)–metabolome (primary producer)–metabolome (secondary producer) continuum. This approach, which is well established and widely used in the research field of human disease (Wang et al. 2022; Yan et al. 2022; Huang et al. 2024), enables us to evaluate the association of the methylome and the sequential mediation through the transcriptome and metabolome, in both primary and secondary producers.

Materials and methods

Culture conditions

The marine diatom *P. tricornutum* Bohlin bac-2, the genome of which is known (Bowler et al. 2008), and is commonly used as model organism for studying the responses of microalgae to global change (Singh et al. 2015; Sabir et al. 2018), was selected as the primary producer. A monoclonal culture of *P. tricornutum*, obtained from the Institute of Oceanology, Chinese Academy of Sciences (No: MASCC-0025, publicly available upon request), was maintained in F/2 solution (Guillard and Ryther 1962) under a photon flux of 100 μmol photons $m^{-2}\,s^{-1}$ with a light : dark cycle of 12 h : 12 h (HP1000G-D, Ruihua) in 15°C plant growth chambers (HP1000G-D, Ruihua). For the long-term adaptation experiments, the single-clone cultures were diluted to separate biological replicates ($n = 3$) and were grown in 500-mL Nalgene bottles at ambient (CO_2: 400 μatm; temperature: 15°C; i.e., the ambient), high CO_2 (CO_2: 1000 μatm; temperature: 15°C), ocean warming (CO_2: 400 μatm; temperature: 20°C), and high CO_2 combined with warming conditions (CO_2: 1000 μatm; temperature: 20°C). The 20°C and 1000 μatm treatment, representing the projected temperature and CO_2 levels at the end of this century, were set according to the high emission scenario SSP5-8.5 (IPCC 2021) in separate plant growth chambers. The photon flux and the light : dark cycle for the long-term adaptation experiments were the same as that of stock cultures (i.e., 100 μmol photons $m^{-2}\,s^{-1}$, light : dark, 12 h : 12 h). Although some previous studies have reported that 20°C is close to the optimal growth temperature of this species (Jiang and Gao 2004; Pérez et al. 2008), our previous work demonstrated that 20°C is a stressor for the strain used in the present study due to strain-specific thermal reaction norms of diatoms (Boyd et al. 2013; Zeng et al. 2020). The CO_2 level of 400 μatm ($\pm$ 30 μatm) was reached by pre-aerating the medium with ambient outdoor air adjusted by the plant growth chamber (HP1000G-D, Ruihua), while the CO_2 level of 1000 μatm was achieved within a plant growth chamber, in which the target CO_2 levels were obtained by mixing air and pure CO_2 gas, and the CO_2 partial pressure was continuously monitored and maintained at 1000 $\pm$ 50 μatm. Three independent replicate semi-continuous batch cultures were run for ~1250 d under the four growth conditions (i.e., ambient, high CO_2, warming, and high CO_2 + warming). The initial cell concentration was 50 cells mL^{-1}, and the cultures were partially renewed every 5–7 d to restore the cell density to the initial level with fresh medium equilibrated with the corresponding target CO_2 levels. The cell densities were maintained within a range of $\sim 4.0 \times 10^4$ to 5.0×10^5 cells mL^{-1} at the time of dilution. To avoid any gas exchange, all the cultures were kept in tightly closed polycarbonate bottles that were filled with culture medium (for details of the carbonate system manipulation, *see* Jin et al. 2022*a*). Because the growth rate of populations in ambient and high-CO_2 conditions was lower than those in warming and its combination with high-CO_2 conditions (Jin et al. 2022*b*), *P. tricornutum* had grown for ~ 2765 and ~ 2758 generations in the former two conditions, and for ~ 2860 and ~ 2815 generations in the latter two conditions after the ~ 1250 d adaptation period.

Feeding experiments

After the ~ 1250 d adaption period, *P. tricornutum* cells under the set conditions were fed to the clam *Coelomactra antiquata* to investigate the food chains effects of high CO_2 and warming in a phytoplankton-clam system. *C. antiquata* is a widely distributed species in the coastal zone of China and has been extensively studied over several decades because of its fast growth rate, ease of artificial propagation, and high

nutritional value (Liu et al. 2006). *C. antiquata* for this study was collected from the coast of Xiamen, China, in October 2022. Approximately, 50 individuals of similar size (6–8 cm) were transported back to the laboratory within 4 h, in a tank of cold water. In the laboratory, each individual was washed with sterile in situ seawater until there were no visible epiphytes on the surface and then starved for at least 24 h before the start of the feeding experiments. In order to avoid any other confounding effects, the feeding experiments were all conducted in 100-liter aquaria with 30 liter in situ seawater under the same ambient conditions (i.e., CO_2: 400 ± 30 μatm; temperature: 20 ± 1°C) with air-bubbling under a photon flux of 100 μmol photons m^{-2} s^{-1} with a light : dark cycle of 12 h : 12 h. Four feeding experiments were conducted independently for 18 d in the present study: (1) clams were fed with ambient-adapted *P. tricornutum* cells; (2) clams were fed with high-CO_2-adapted *P. tricornutum* cells; (3) clams were fed with warming-adapted *P. tricornutum* cells; (4) clams were fed with high-CO_2- and warming-adapted *P. tricornutum* cells. In each feeding experiment, 30 liters in situ seawater were renewed every 24 h to avoid any large environmental variabilities (such as nutrient concentrations) in the middle of the light period, and ~ 12 individuals were fed with 1 liter pre-adapted cultures ($\sim 4.0 \times 10^5$ cells mL^{-1}, i.e., a total cell number of 8.0×10^8) after renewal of the seawater. The feces of the clams were removed and disposed of every day. Seawater samples (1 liter) in the aquaria were collected before the feeding of algae to count the cell densities and then to assess the consumption of the diatom *P. tricornutum* by the clam *C. antiquata* (> 98% in all the four feeding experiments, data not shown). The temperature was controlled by a water bath and maintained at 20 ± 1°C (Supplementary Fig. S1). The pH changes were measured at the beginning, middle, and the end of the light phase every day with a PB-10 pH meter (Sartorius) which was calibrated with standard National Bureau of Standards (NBS) buffer solution (Hanna; mean pH: 8.05 ± 0.02 throughout the experiment; Supplementary Fig. S2). The dissolved oxygen concentration and the salinity of the seawater in aquaria were monitored by a MultiLab 4010-1W (YSI, Achalaich) and a portable refractometer WZ201, respectively, in parallel with pH three times per day throughout the whole experiment (Supplementary Figs. S3, S4). All the 12 individuals in each feeding experiment grew well, and no individual died. At the end of the feeding experiments, the clams were cleaned with sterile seawater and the adductor muscle tissues were removed quickly and entirely from the shell, frozen in liquid nitrogen, and stored at −80°C for further analysis.

Multi-omics sequencing and data processing

To avoid any temporal or diurnal effects, all the samples taken for transcriptome and DNA methylation analysis were collected in the middle of the light phase at the same adaptation time point of 2 yr. Specifically, the transcriptome analysis of *P. tricornutum* was performed with three biological replicate samples collected after the *P. tricornutum* cultures had been grown under ambient, high CO_2, warming, and its combination with high-CO_2 conditions for 2 yr as described in Jin et al. (2022*b*). Briefly, cells were harvested in the middle of the photoperiod by centrifugation ($8000 \times g$, 10 min), and the samples were then flash-frozen in liquid nitrogen and stored at −80°C until further analysis. Total RNA was extracted using a Trizol reagent kit (Invitrogen) according to the manufacturer's protocol. RNA quality was assessed on an Agilent 2100 Bioanalyzer (Agilent Technologies) and checked using RNase-free agarose gel electrophoresis. RNA libraries were prepared as described in Jin et al. (2022*b*), and sequenced using NovaSeq 6000 by Gene Denovo Biotechnology Company. The reads obtained from the sequencing machines were quality-checked using fastp (version 0.18.0; Chen et al. 2018). Filtered reads were mapped to the *P. tricornutum* genome (Bowler et al. 2008) using HISAT (Kim et al. 2015, version 2.2.1), after ribosomal RNA (rRNA)-mapped reads were removed from the reference genome fasta file (Langmead and Salzberg 2012). Counting and normalization of mapped reads and analysis of differential expression were done as previously described in Jin et al. (2022*b*).

For the DNA methylation analysis, *P. tricornutum* cells grown under ambient, high CO_2, warming, and high CO_2 + warming conditions for 2 yr were also harvested in the middle of the photoperiod by centrifugation ($8000 \times g$, 10 min). The genomic DNA was extracted using a plant genomic DNA kit following the manufacturer's instructions. The DNA integrity and concentration were measured by agarose gel electrophoresis and NanoDrop spectrophotometer, respectively. Following this, DNA libraries for bisulfite sequencing were prepared as described in Wan et al. (2023). The reads with more than 10% of unknown nucleotides (N) and that with more than 40% of low quality (Q-value ≤ 20) were removed from the raw reads for quality check. Filtered reads were mapped to the *P. tricornutum* genome (Bowler et al. 2008) using BSMAP software (version: 2.90) by default (Xi and Li 2009). A custom Perl script was used to identify methylated cytosines and the methylated cytosines were tested with the correction algorithm as described in Lister et al. (2009). Differential DNA methylation between two populations under different conditions (e.g., ambient vs. high CO_2) at each locus were determined using Pearson's chi-square test (χ^2) in methylKit (Akalin et al. 2012, version: 1.7.10). To identify differentially methylated cytosines (DMCs), the minimum read coverage to call a methylation status for a base was set to 4. DMCs for each sequence context (CG, CHG, and CHH) between two populations under different conditions were identified using specific criteria. For CG, a difference in methylation ratio with an absolute value of ≥ 0.25 and a q-value of ≤ 0.05 was required. For CHG, the difference in methylation ration had to have an absolute value of ≥ 0.25 and a q-value of ≤ 0.05. For CHH, the difference in methylation ratio had to have an absolute value of ≥ 0.15 and a q-value of ≤ 0.05. For all C, the

difference in methylation ratio had to have an absolute value of ≥ 0.2 and a q-value of ≤ 0.05.

Metabolites profiling and data processing

After the ~1250 d adaption period, six replicate samples ($n = 6$), accounting for the inherently greater variability associated with metabolomic analyses, of *P. tricornutum* cells grown under ambient, high CO_2, warming, and its combination with high CO_2 were collected in the middle of the photoperiod, centrifuged (8000 × g, 10 min), flash frozen in liquid nitrogen, and stored at −80°C until metabolite analysis. For the metabolite extractions, the harvested cells of *P. tricornutum* and the tissue of clams were washed with sterile seawater at 37°C and the sterile seawater then removed. Then, 800 μL of cold methanol/acetonitrile (1 : 1, v/v) was added to remove the protein and extract the metabolites. The mixture was collected into a new centrifuge tube, and centrifuged (14,000 × g, 5 min) to collect the supernatant. The supernatant was then dried in a vacuum centrifuge. For LC–MS analysis, the samples were re-dissolved in 100 μL acetonitrile/water (1 : 1, v/v). To monitor the stability and repeatability of the analysis, quality control (QC) samples were prepared by pooling 10 μL of each sample and analyzed together with the other samples. The QC samples were inserted regularly and analyzed in every five samples (Supplementary Fig. S4).

LC–MS/MS analysis was performed using an ultrahigh-performance liquid chromatography (UHPLC, 1290 Infinity LC, Agilent Technologies) coupled to a quadrupole time-of-flight mass spectrometer (AB Sciex TripleTOF 6600) at Shanghai Applied Protein Technology Co., Ltd. For hydrophilic interaction liquid chromatography (HILIC) separation, samples were analyzed using a 2.1 mm × 100 mm ACQUIY UPLC BEH 1.7-μm column (Waters, Ireland). The column temperature was set at 25°C. A 2 μL aliquot of each sample was injected for the analysis. The mobile phase buffer A was 25 mM ammonium acetate and 25 mM ammonium hydroxide, whereas buffer B was acetonitrile. The solvent gradient was set as follows: 95% buffer B, 0–0.5 min; 95–65% buffer B, 0.5–7 min (a linear decrease); 65–40% buffer B, 7–8 min (a linear decrease); 40% buffer B, 8–9 min; 40–95% buffer B, 9–9.1 min (a linear increase); 95% buffer B, 9.1–12 min. The electrospray ionization (ESI) source conditions were set as follows: Ion Source Gas1 (Gas1) as 60, Ion Source Gas2 (Gas2) as 60, curtain gas (CUR) as 30, source temperature at 600°C, IonSpray Voltage Floating (ISVF) ± 5500 V. In MS only acquisition, the instrument was set to acquire over the m/z 60–1000 Da scanning range, and the accumulation time for TOF MS scan was set as 0.20 s spectra^{-1}. In the auto MS/MS acquisition model, the scanning range was set as m/z 25–1000 Da, and the accumulation time was 0.50 s spectrum^{-1}. The product ion scan was acquired using information dependent acquisition (IDA) with high-sensitivity mode selected. The parameters were set as follows: the collision energy (CE) was fixed at 35 V with ± 15 eV; declustering potential (DP) was set as ± 60 V; exclude isotopes within 4 Da, and the candidate ions to monitor per cycle was set as 10. Low-quality ions (ions that were missing in over 50% of quality control samples or over 80% of test samples), or ions with relative standard deviation > 30%, were excluded for downstream analysis (Dunn et al. 2011). In the extracted ion features, only the variables having more than 50% of the nonzero measurement values in at least one group were kept. Compound identification of metabolites was performed by comparison of the accuracy of the m/z value (< 10 ppm), and MS/MS spectra with an in-house database established with available authentic standards.

After metabolic information collection and data preprocessing, we first applied the multivariate beta-diversity analyses of permutational multivariate ANOVA (PERMANOVA) and analysis of similarities (ANOSIM) to test the metabolomics profile differences among groups (e.g., ambient vs. high CO_2). To extract and visualize the metabolomics profile differences between groups, we used principal component analysis (PCA), principal coordinates analysis (PCoA), and nonmetric multidimensional scaling (NMDS). The similarity index was set to Bray–Curtis and we used 9999 for the permutation N. Since the metabolomic analyses exhibited inherently greater variability compared to other omics data, NMDS and PCoA were not adopted for the visualization in the present study (data not shown). Subsequently, we decided to use the dimensionality reduction method of orthogonal partial least squares discriminant analysis (OPLS-DA) to distinguish the metabolomics profile of two groups by screening variables correlated to class memberships (Worley and Powers 2013; Roede et al. 2014). Identification of metabolites has a variable importance in the projection (VIP) graphs (99% confidence; Roede et al. 2014). For each multivariate model, the calculated R^2 value reflects the goodness of fit. The parameter $Q2$ in the PLS-DA represents the predictive ability of the model (Roede et al. 2014). A $Q2$ value close to 0.5 reflects a good model. We applied univariate analysis (t-test) to calculate the statistical significance (p-value). Metabolites with VIP ≥ 1, $p < 0.05$ were considered to be differential metabolites. However, due to the nature of the methodology applied, we were not able to identify the absolute cellular contents of the differential metabolites.

The Kyoto Encyclopedia of Genes and Genomes (KEGG) database was used for enrichment analysis and pathway analysis of differential metabolites. Metabolites were mapped to KEGG metabolic pathways for annotation and enrichment analysis. Pathway enrichment analysis identified significantly enriched metabolic pathways or signal transduction pathways in differential metabolites comparing with the whole background. The formula for calculations is as follows:

$$P = 1 - \sum_{i=0}^{m-1} \frac{\binom{M}{i}\binom{N-M}{n-i}}{\binom{N}{n}}$$

where N is the number of all metabolites with KEGG annotation, n is the number of differential metabolites in N, M is the number of all metabolites annotated to specific pathways, and m is number of differential metabolites in M. Here, we define the calculated p-value that was subjected to false discovery rate (FDR) correction as a Q-value, taking $Q \leq 0.05$ as a threshold. Pathways meeting these criteria were defined as significantly enriched pathways with differential metabolites. Pathways with $p \leq 0.05$ but $Q > 0.05$ were also considered as significantly enriched metabolic pathways in the present study.

Integrative multi-omics analysis

We hypothesized that the changes of DNA methylation in *P. tricornutum* may act cooperatively with gene transcription, which may regulate the biosynthesis or metabolism of its metabolites and then alter its food quality, and thereby alter the metabolite compositions of the consumers that fed with *P. tricornutum* cells (i.e., clams in the present study). To test this hypothesis, we conducted a sequential mediation analysis for multi-omics KEGG pathways along the methylome (diatom)–transcriptome (diatom)–metabolome (diatom)–metabolome (clam) axis (MethD–TranD, TranD–MetaD, MetaD–MetaC), to assess the association of the methylome that was sequentially mediated through the transcriptome, metabolome both in diatoms and their clam consumers (Yan et al. 2022). The mediation analysis between sequential pairs of omics pathways was performed using the R mediate package.

Results

Metabolomic signatures of diatoms to high CO_2 and/or warming adaptation

The liquid chromatography with tandem mass spectrometry (LC–MS/MS) produced 14,483 unique metabolite features, of which 783 had a spectral match to a known compound in the in-house database established with available authentic standards. The total metabolome showed strong differentiation between long-term high CO_2 and its combination with warming-adapted and non-adapted populations (PERMANOVA, high CO_2: $R^2 = 0.39$, $p = 0.005$; high CO_2 + warming: $R^2 = 0.39$, $p = 0.004$; ANOSIM, high CO_2: $R = 0.72$, $p = 0.002$; high CO_2 + warming: $R = 0.66$, $p = 0.003$; Fig. 1). However, the warming-adapted populations did not show a significant differentiation of the total metabolome from that of non-adapted populations (PERMANOVA, $R^2 = 0.14$, $p = 0.134$; Fig. 1). The results revealed that 90 and 7 metabolites with known identities had significantly higher and lower abundance, respectively, in long-term high-CO_2-adapted

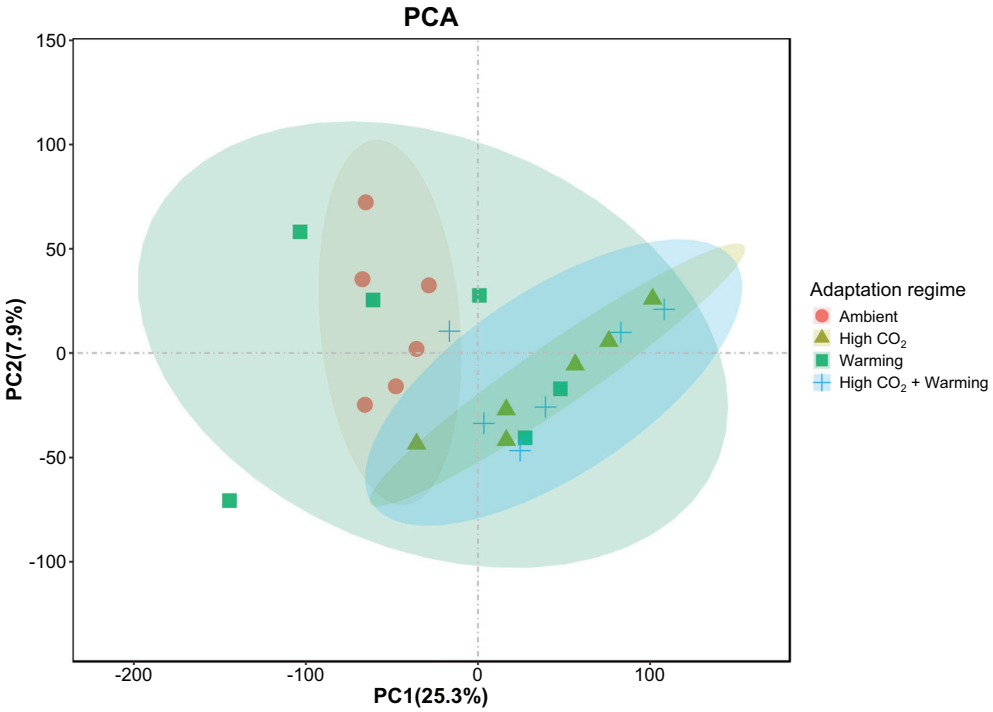

Fig. 1. Principal component analysis (PCA) of metabolites among diatoms in different adaptation regimes. Diatoms in different adaptation regimes are shown in different colors and shapes ($n = 6$). The ellipses in PCAs give the 95% confidence interval around the centroid and thus give an idea of whether the metabolites in diatoms in different adaptation regimes differ significantly.

P. tricornutum cells when compared to those of cells grown in ambient conditions (criteria given in the "Materials and methods" section, i.e., metabolites with VIP ≥ 1, $p < 0.05$; Table 1; Supplementary Table S1). For the long-term warming-adapted *P. tricornutum* cells, 28 and 30 metabolites with known identities had significantly higher or lower abundance, respectively (Table 1; Supplementary Table S1). For the changes in metabolites in *P. tricornutum* cells adapted under high CO_2 combined with warming, 87 higher abundance and 18 lower abundance known metabolites were observed (Table. 1; Supplementary Table S1). We then used the variable importance in the projection (VIP; for details, *see* "Materials and methods" section) to identify the most important compounds for discriminating between adapted and non-adapted cells. This analysis revealed that purine nucleosides (e.g., adenosine), glycerophospholipids, prenol lipids, organonitrogen compounds, and organooxygen compounds were the most important classes for distinguishing the long-term high-CO_2-adapted cells (Fig. 2a; Supplementary Fig. S5). Carboxylic acids and derivatives, organonitrogen compounds, hydroxy acids and derivatives, steroids and steroid derivatives, and prenol lipids were the most important classes for distinguishing the long-term warming-adapted cells (Fig. 2b; Supplementary Fig. S5). For the cells adapted under high CO_2 combined with warming conditions, naphthofurans, organonitrogen compounds, yohimbine alkaloids, glycerophospholipids, coumarins and derivatives, organooxygen compounds, and prenol lipids were the most important classes (Fig. 2c; Supplementary Fig. S5). These results indicate that long-term adaptation to high CO_2 and/or warming significantly altered the metabolome of *P. tricornutum* populations.

By mapping the annotated metabolites to the KEGG database, 36 known metabolites with differential abundance in high-CO_2-adapted *P. tricornutum* were annotated with 63 KEGG pathways (Supplementary Table S2). Among these pathways, five (arginine and proline metabolism, carbapenem biosynthesis, C5-branched dibasic acid metabolism, taurine and hypotaurine metabolism, and porphyrin and chlorophyll metabolism) exhibited significant enrichment ($Q \leq 0.05$; Supplementary Table S2). In the long-term warming-adapted cells, 14 known metabolites with differential abundance were annotated with 47 KEGG pathways. However, none of these pathways showed significant enrichment ($Q > 0.05$; Supplementary Table S3). Thirty known metabolites with differential abundance in the long-term high-CO_2- and warming-adapted cells were annotated with 47 KEGG pathways. Notably, two pathways, namely carbapenem biosynthesis and porphyrin and chlorophyll metabolism, exhibited significant enrichment ($Q \leq 0.05$; Supplementary Table S4).

Table 1. Summary of the numbers of metabolites with differential abundance in *Phaeodactylum tricornutum* populations in long-term CO_2 and/or warming conditions compared with that under ambient conditions.

	Number of differential metabolites	Number of upregulated metabolites	Number of downregulated metabolites
High CO_2	97	90	7
Warming	58	28	30
High CO_2 + warming	105	87	18

Metabolomic signatures of clams feeding on diatoms under different adaptation regimes

In order to test whether the metabolite changes in diatoms would be transferred via the food chain to alter the metabolite composition and/or abundance in clams feeding on diatoms under different adaptation regimes (i.e., ambient, high CO_2, warming, high CO_2 + warming), we adopted the LC–MS/MS approach to identify the metabolites with differential abundance in clams. For the analysis, LC–MS/MS produced 22,182 unique metabolite features, of which 1341 had a spectral match to a known compound in the in-house database. Different from that of diatoms, the total metabolome of clams did not show strong differentiation between clams feeding on adapted and non-adapted (i.e., ambient) diatoms (PERMANOVA, high CO_2: $R^2 = 0.14$; warming: $R^2 = 0.10$; high CO_2 + warming: $R^2 = 0.15$; all $p > 0.05$; ANOSIM, high CO_2: $R = 0.137$; warming: $R = 0.052$, high CO_2 + warming: $R = 0.172$; all $p > 0.05$; Fig. 3). We identified 6 and 30 metabolites with known identities showing significantly higher and lower abundance, respectively, in clams feeding on long-term high-CO_2-adapted *P. tricornutum* cells compared to clams feeding on diatoms grown in ambient conditions (criteria given in "Materials and methods" section, i.e., metabolites with VIP ≥ 1, $p < 0.05$; Table 2; Supplementary Table S5). In the case of clams feeding on diatoms in the long-term warming regimes, we found 16 and 46 metabolites with known identities exhibiting significantly higher and lower abundance, respectively (Table 2; Supplementary Table S5). Moreover, when clams were fed on diatoms grown in high-CO_2 and warming conditions, we identified 25 and 63 known metabolites with significantly higher and lower differential abundance, respectively (Table 2; Supplementary Table S6). As with the diatoms, we identified the most important compounds for discriminating between clams feeding on adapted and non-adapted cells by the VIP index. The results showed that organic sulfonic acids and derivatives (e.g., guanidinoethyl sulfonate, taurine), glycerophospholipids, fatty acyls, heteroaromatic compounds, and carboxylic acids and derivatives (e.g., glycine) were the most important classes for distinguishing the clams feeding on long-term high-CO_2-adapted diatoms (Fig. 4a; Supplementary Fig. S6). In the case of clams feeding on diatoms in long-term warming regimes, fatty acyls, keto acids and derivatives, organic sulfonic acids and derivatives (e.g., taurine), organonitrogen compounds, sulfoxides,

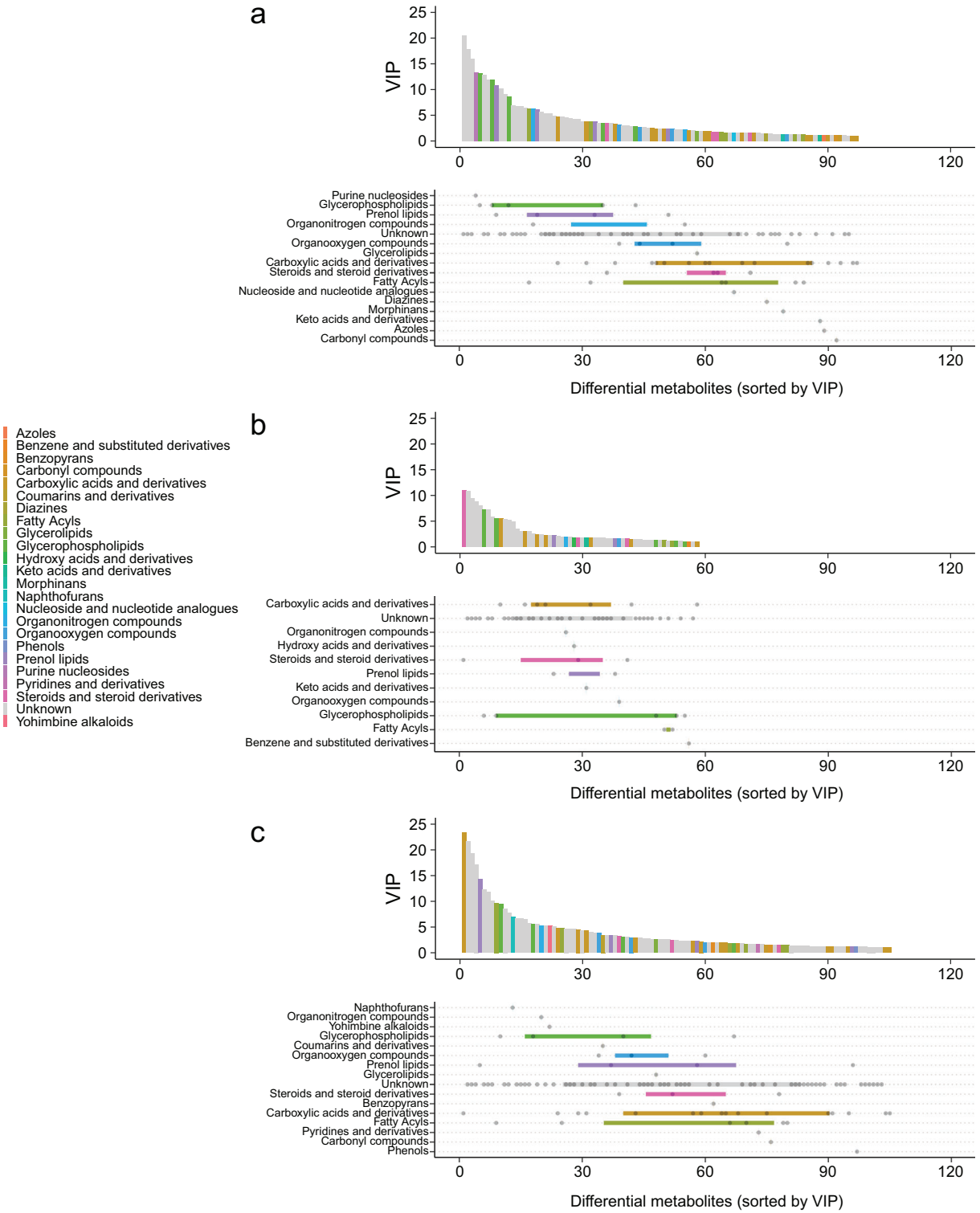

Fig. 2. Metabolomic signatures of diatoms to high CO_2 and/or warming adaptation. Variable importance in the projection (VIP) ranking of differential metabolites (bar plot) and importance ranking of metabolites classes (horizontal box plot) in long-term high CO_2 (**a**), warming (**b**), and its combination with high-CO_2-adapted populations (**c**). Individual points in horizontal box plots correspond to ranked metabolites in bar plots (lower is more informative), with horizontal bars showing the 1st and 3rd quartiles of each molecular family. Colors in the horizontal box plots correspond to molecular classes in the bar plots. Boxes represent the interquartile range (IQR).

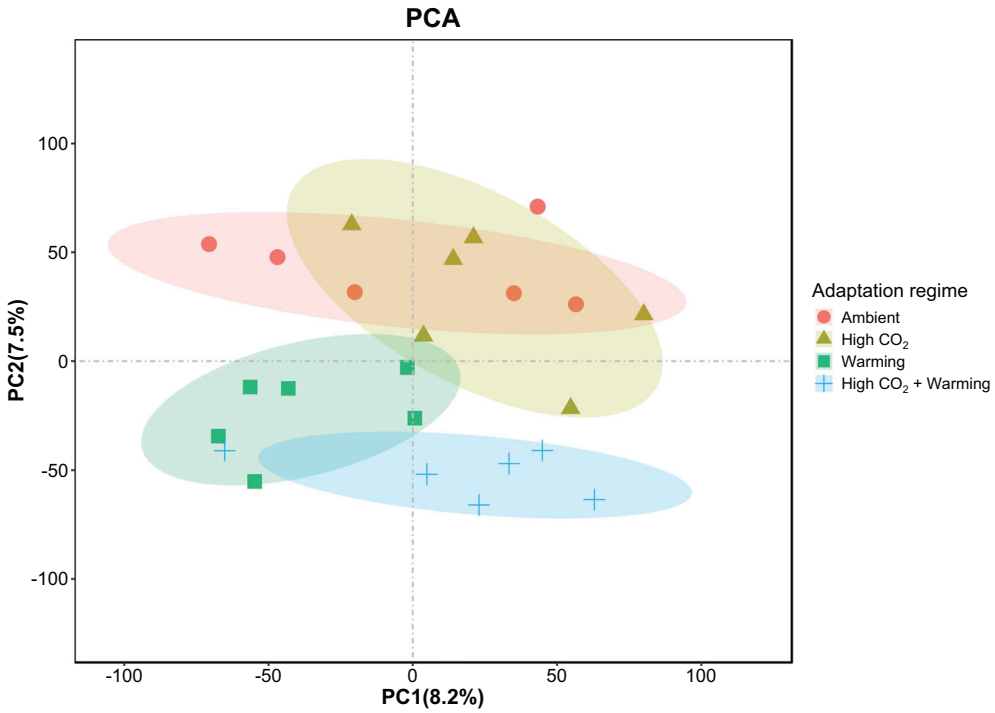

Fig. 3. Principal component analysis (PCA) of metabolites among clams feeding on diatoms under different adaptation regimes. Clams feeding on diatoms under different adaptation regimes are shown in different colors and shapes ($n = 6$). The ellipses in PCAs give the 95% confidence interval around the centroid and thus give an idea of whether the metabolites in clams feeding on diatoms under different adaptation regimes differ significantly.

Table 2. Summary of the numbers of metabolites with differential abundance in *Coelomactra antiquata* that were fed with long-term CO_2 and/or warming-adapted *Phaeodactylum tricornutum* cells when compared with that were fed with long-term ambient-adapted ones.

	Number of differential metabolites	Number of upregulated metabolites	Number of downregulated metabolites
High CO_2	36	6	30
Warming	62	16	46
High CO_2 + warming	88	25	63

and piperidines were the most important classes (Fig. 4b; Supplementary Fig. S6). For the clams feeding on diatoms in long-term high CO_2 and warming regimes, organic sulfonic acids and derivatives (e.g., guanidinoethyl sulfonate, taurine), phenols, sulfoxides, fatty acyls, glycerophospholipids, and piperidines were the most important classes (Fig. 4c; Supplementary Fig. S6). Taken together, our results suggest that the changes in metabolomic profile in the primary producer (diatoms) can be transferred to a secondary producer (clams), resulting in significant changes in abundance of certain metabolites.

Upon mapping the annotated metabolites to the KEGG database, we identified 11 known metabolites with differential abundance in clams feeding on high-CO_2-adapted diatoms, and these were annotated with 33 KEGG pathways. Out of these pathways, only one pathway, namely protein digestion and absorption, exhibited significant enrichment ($Q \leq 0.05$; Supplementary Table S6). For clams feeding on warming-adapted diatoms, 27 known metabolites with differential abundance were annotated with 77 KEGG pathways. Surprisingly, none of these pathways showed significant enrichment ($Q > 0.05$; Supplementary Table S7). The same lack of significant enrichment was also observed for clams feeding on high CO_2 + warming-adapted diatoms, where 31 known metabolites with differential abundance were annotated with 40 pathways (Supplementary Table S8).

Integrated multi-omics for diatom–clam interactions

The results presented above indicated that metabolites changes in diatoms would transfer via the food chain to alter the metabolite composition and/or abundance in clams feeding on diatoms grown under different adaptation regimes. Then we further hypothesized the metabolite changes in diatoms may be regulated by gene transcription, which in turn might be modified by DNA methylation. To test this hypothesis, we conducted a sequential mediation analysis for multi-omics KEGG pathways along the methylome (diatom)–transcriptome (diatom)–metabolome (diatom)–metabolome (clam) axis (MethD–TranD, TranD–MetaD, MetaD–MetaC), to

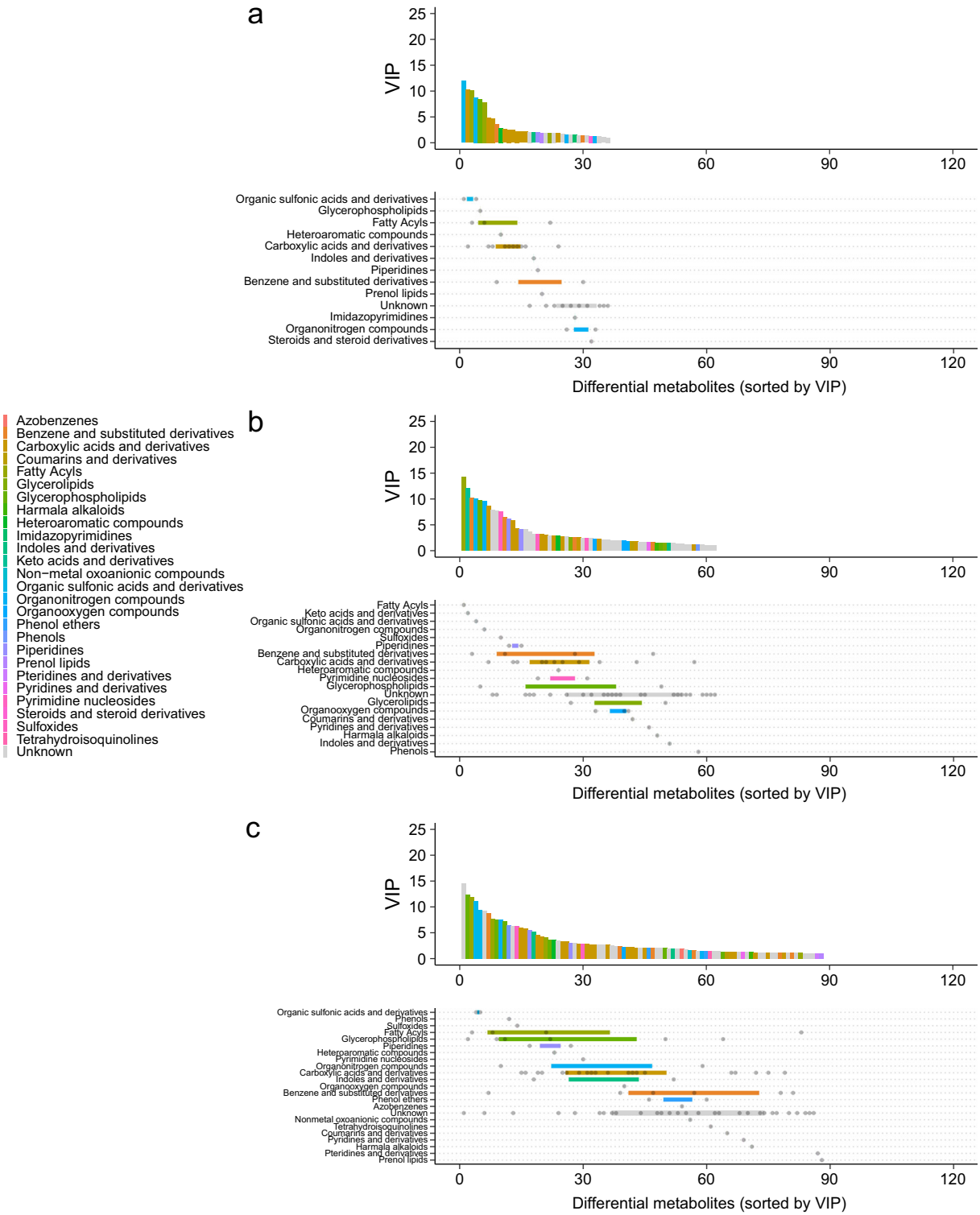

Fig. 4. Metabolomic signatures of clams feeding on diatoms under different adaptation regimes. Variable importance in the projection (VIP) ranking of differential metabolites (bar plot) and importance ranking of metabolites classes (horizontal box plot) in clams feeding on long-term high CO_2 (**a**), warming (**b**), and its combination with high-CO_2-adapted populations (**c**). Individual points in horizontal box plots correspond to ranked metabolites in bar plots (lower is more informative), with horizontal bars showing the 1st and 3rd quartiles of each molecular family. Colors in the horizontal box plots correspond to molecular classes in the bar plots. Boxes represent the interquartile range (IQR).

assess the association of methylome that was sequentially mediated through the transcriptome and metabolome both in the diatoms and the clams feeding on them.

For the *P. tricornutum* methylome and transcriptome, all 10,395 (refer to its reference genome) and 10,656 genes (refer to its reference genome and new genes by transcriptome) were

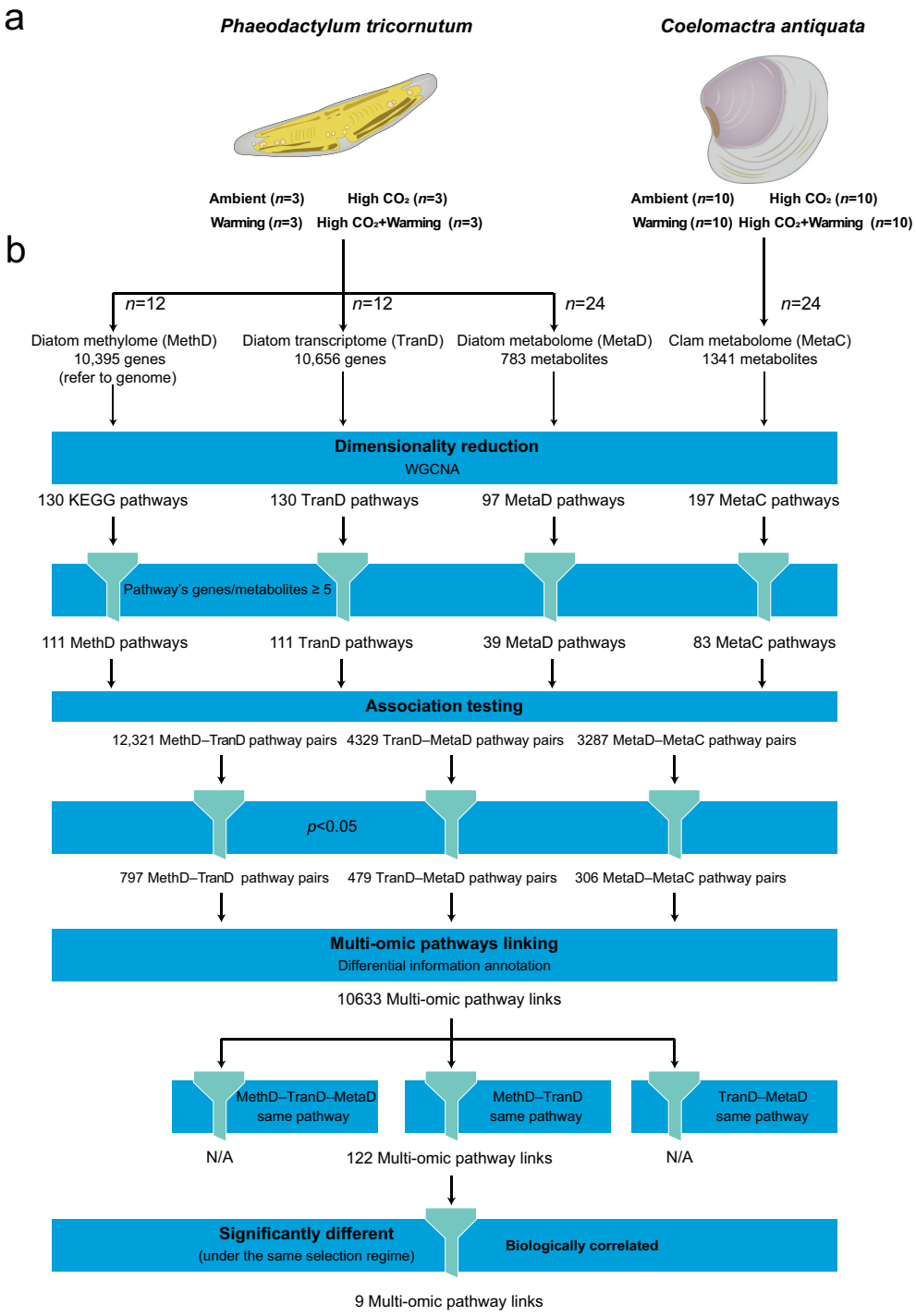

Fig. 5. The overall workflow integrating multi-omics reveals signatures of metabolite transfers from the primary producer to the secondary producer. To identify the biological links between primary (diatom) and secondary producers (clam), a sequential mediation analysis was performed along the methylome (diatom)–transcriptome (diatom)–metabolome (diatom)–metabolome (clam) axis (MethD–TranD, TranD–MetaD, MetaD–MetaC), to assess the association of the methylome that was sequentially mediated through the transcriptome to the metabolome, both in diatoms and their consumer clam. Cross-omic biological links were then identified from pairs of pathways with significant mediation effects (Spearman correlation test, $p \leq 0.05$).

binned into the 130 KEGG pathways by using BLASTx program (http://www.ncbi.nlm.nih.gov/BLAST/) with an *E*-value threshold of 10^{-5} to the KEGG database (http://www.genome.jp/kegg; Fig. 5). Of these, the pathways with no less than 5 genes (that was 111 pathways) were further used for the sequential mediation analysis (Fig. 5). The untargeted metabolomics identified 783 and 1341 metabolites of known identity in diatoms and clams, respectively (Fig. 5). Then these numbers of metabolites were binned into 97 (MetaD) and 197 (MetaC) KEGG pathways by pathway annotation, respectively (Fig. 5). As was done for that of MethD and TranD, the pathways with no less than 5 metabolites were further used for the sequential mediation analysis, and these resulted in 39 and 83 pathways in MetaB and MetaC, respectively (Fig. 5). Then, 12,321, 4329, and 3287 pathway pairs were identified in the pairs of MethD–TranD, TranD–MetaD, and MetaD–MetaC, respectively, based on the pathway eigengene by weighted correlation network analysis (WGCNA). Out of these pathway pairs, only 797 (6.5%), 479 (11.1%) and 306 (9.3%) pairs were identified with significant mediation effects (Spearman correlation test, $p \le 0.05$). The multi-omics mediation effects were stronger for TranD–MetaD and MetaD–MetaC compared with MethD–TranD, implying a more intense transcriptome–metabolome and metabolome (diatom)–metabolome (clam) association. These significant pairs resulted in 10,633 multi-omics pathway links in total (Fig. 5).

Among the 10,633 multi-omic pathway links explored, no shared pathway was identified through the MethD–TranD–MetaD or the TranD–MetaD under any of the adaptation regimes (Fig. 5). However, we observed 122 shared multi-omic pathway links in the MethD–TranD pair (Fig. 5; Supplementary Fig. S7). Within these shared pathways, only nine were found to have significant mediation effects (Spearman correlation test, $p \le 0.05$) under the warming adaptation regime (Fig. 6; Supplementary Table S9). In these nine pathways, we found that the downregulated terpenoid backbone

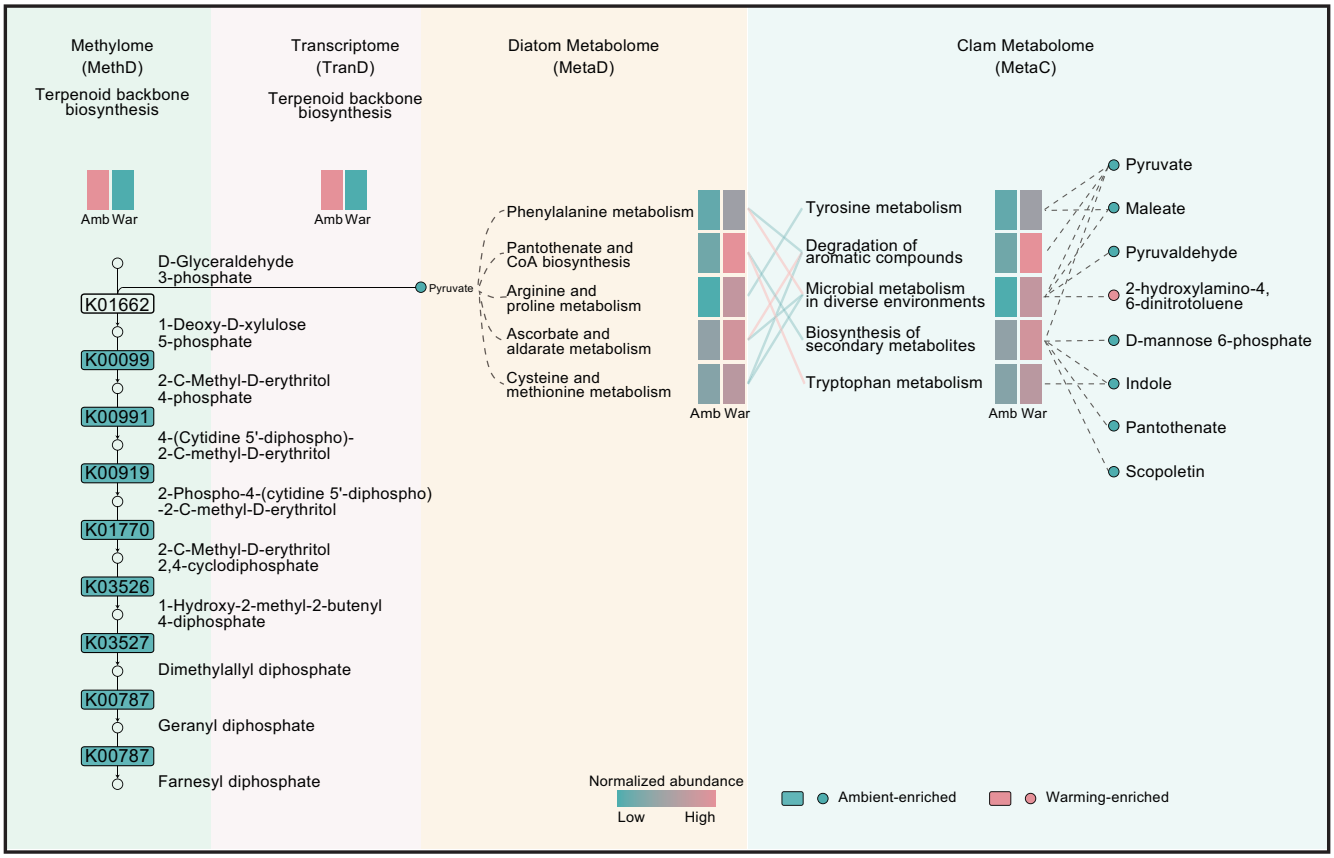

Multi-omic biological links

Fig. 6. Multi-omics biological links for diatom-clam interactions. The KOs in the pairs MethD–TranD, TranD–MetaD, MetaD–MetaC with significant mediation effects under the warming adaptation regime compared to that under ambient regime are shown (Spearman correlation test, $p \le 0.05$). The direction of alteration of KOs (rectangles) or metabolites (cycles) are shown by color (red: up, blue: down). Pathways with significant correlation are connected by colored lines (red: positive correlation; blue: negative correlation). The heatmaps display the changes in the normalized abundance of metabolites between diatoms under ambient (Amb) and warming regime (War) or clams feeding on diatoms under ambient regime (Amb) and warming regime (War).

biosynthesis pathway in MethD was linked to the same pathway in TranD (also downregulated) under the warming adaptation regime (Fig. 6; Supplementary Fig. S7). Subsequently, the terpenoid backbone biosynthesis pathway was linked to pyruvate (with lower abundance in warming regime compared with that under ambient regime, 79.7%), which, in turn, was linked to upregulated pathways of phenylalanine metabolism, pantothenate and CoA biosynthesis, arginine and proline metabolism, ascorbate and aldarate metabolism, and cysteine and methionine metabolism in MetaD (Fig. 6; Supplementary Fig. S8). In addition, we observed that these five pathways were further linked to the upregulated pathways in MetaC, including tyrosine metabolism, degradation of aromatic compounds, microbial metabolism in diverse environments, biosynthesis of secondary metabolites, and tryptophan metabolism (Fig. 6; Supplementary Fig. S9). Metabolites such as pyruvate, maleate, pyruvaldehyde, D-mannose 6-phosphate, indole, pantothenate, and scopoletin, which are involved in these five upregulated pathways, were found to have significantly lower abundance in warming regime compared with that under ambient regime (27.66–52.37%; Fig. 6). Conversely, the abundance of 2-hydroxylamino-4,6-dinitrotoluene was significantly higher in warming regime (173.14%; Fig. 6). These results collectively form a mechanistic hypothesis: under the warming adaptation regime, the downregulated terpenoid backbone biosynthesis in the methylome and transcriptome may lead to decreased pyruvate levels and upregulation of some pathways (such as phenylalanine metabolism) in the metabolome of diatoms. This altered metabolomic profile could then be transferred to clams, leading to changes in the abundance of certain metabolites, such as decreases in pyruvate and pyruvaldehyde and increases in other metabolites such as 2-hydroxylamino-4,6-dinitrotoluene (Fig. 6). To summarize, our results indicate that the signatures of trophic transfer from primary producer to secondary producer can be reflected across different levels of biological organization.

Discussion

Our data demonstrate a strong metabolomic signature of long-term adaptations of a marine diatom to long-term high CO_2 and/or warming. When subjected to long-term high CO_2 and its combination with warming conditions, notable shifts were observed in metabolic pathways, particularly in carbapenem biosynthesis, porphyrin, and chlorophyll metabolism (Fig. 2; Supplementary Table S1). Notably, metabolites such as pheophorbide *a*, canthaxanthin, and abscisic acid exhibited significantly augmented levels (Fig. 2; Supplementary Table S1). It is known that microalgae increase the production of abscisic acid in response to various abiotic factors (e.g., heat, light, drought; Bajguz 2009; Hartung 2010), and specifically, that abscisic acid can accelerate the recovery of PSII complex from damage by photoinhibition (Saradhi et al. 2000). In parallel with abscisic acid, canthaxanthin, which is well recognized as a natural antioxidant compound that scavenges free radicals and decreases oxidative damage (Esabyoglou and Rimbach 2017), was more abundant in cells adapted to the long-term high-CO_2 condition and its combination with warming (Fig. 2; Supplementary Table S1). These results suggest that the marine diatom *P. tricornutum* is likely to be suffer oxidative damage after long-term exposure to high CO_2 and its combination with warming conditions. This hypothesis was further supported by the enhanced level of proline (Fig. 2; Supplementary Table S1), which is considered to act as a compatible osmolyte and to function as a protector of macromolecules in response to oxidative damage (Szabados and Savouré 2010), in all the adaptation regimes (i.e., high CO_2, warming, high CO_2 + warming). This finding is in good agreement with some previous studies, which demonstrated that increased levels of CO_2 enhanced the accumulation of proline that may limit oxidative damage (Xu et al. 2019; Moreno et al. 2023). Furthermore, phytoplankton increase their lipid content, which may mitigate oxidative damage and decrease the saturation of lipids under warming condition (Jin et al. 2020; Holm et al. 2022; Leles and Levine 2023). It is worth noting that due to the nature of the metabolomics approach applied in the present study, little information can be obtained regarding the absolute cellular contents of each metabolite with significant abundance, and this issue should be carefully addressed in future investigations. In summary, our results suggest that the alterations in specific metabolites, such as abscisic acid and proline, in the long-term high-CO_2- and/or warming-adapted diatom provide potential for their use as biomarkers for unraveling the biological mechanisms underlying the adaptation of phytoplankton to changing marine environmental conditions in the context of global change.

In addition to effects on the diatoms, our results showed distinct metabolite profiles in clams feeding on diatoms across different adaptation regimes. Notably, the abundance of γ-aminobutyric acid (GABA), a non-proteinogenic amino acid comprising four carbons and serving as the principal inhibitory neurotransmitter in vertebrates' central and peripheral nervous systems and also functions in the nervous system of bivalves such as clams (Jessen et al. 1979; Chen et al. 2021), exhibited an increase in clams feeding on long-term warming-adapted diatoms (Fig. 4; Supplementary Table S5). Environmental perturbations, such as elevated CO_2, can disrupt neural signal transmission through GABA–GABA receptors, and then affect behavior, for example, the feeding activity of bivalves (Nilsson et al. 2012; Peng et al. 2017). Therefore, the accumulation of GABA in clams feeding on long-term warming-adapted diatoms hints at potential disruptions in their neural signal transmission. However, we did not observe an obvious change in feeding rates of clams that were fed on diatoms across different adaptation regimes, suggesting that the effects of GABA on feeding behavior of clams might be diminished in

the present study. At the same time, the abundance of pyruvaldehyde, a toxic ubiquitous metabolite that affects redox homeostasis (Kumar et al. 2021), was found to decrease in clams feeding on long-term warming-adapted diatoms (Fig. 4; Supplementary Table S5). How would this affect the clams' behavior and its potential ecological consequences remains to be explored.

In contrast to the increased abundance of GABA, the abundance of the metabolite taurine was found to decrease in clams feeding on long-term high CO_2 and/or its combination with warming-adapted diatoms (Fig. 4; Supplementary Table S5). Taurine, which is a significant organic osmolyte in bivalves, was considered to play a vital role in their thermal responses to increasing temperature (Yancey 2005; Stickle et al. 2010; Gleason et al. 2017). It is believed that taurine contributes to stabilizing protein structures against thermal denaturation, maintaining their native and active states without alterations in protein concentration (Arakawa and Timasheff 1985). Therefore, our findings imply that not only the environmental perturbations, but also the nutritional quality of primary producers they induced, would alter the metabolite profiles of secondary producers, and has the potential to have profound consequences for marine ecosystem and seafood quality as a result of progressive ocean changes.

This study has several limitations. First, we conducted a sequential mediation analysis with the multi-omics data and then identified the biological links across different levels of biological organization from primary producers to secondary producers. This approach may not fully elucidate complex mechanisms, for instance, the effects of regulation of certain genes or DNA methylation or metabolites in primary producers on the abundances of some key metabolites in secondary producers. Second, the metabolite profile changes in clams may have the potential to influence aspects of their behavior, such as burrowing, feeding and reproduction, which were not fully determined in the present study. These effects and their ecological consequences need to be further assessed. Third, the feeding experiments with secondary producers were conducted over a relatively short term ($\sim$ 20 d) period, compared to the adaptation experiments with the primary producers ($\sim$ 4 yr), and this will not allow us to examine the adaptation capacity of secondary producers with different food sources. Such a food chain effect at a long-term adaptation scale cannot be ignored in future investigations. Finally, although we did not identify any high variabilities of various environmental parameters (such as pH, dissolved oxygen) throughout the feeding experiments, we recognize that measuring additional environmental parameters such as nutrients (N, P) could have allowed us to better understand the nutrient dynamics in the system, which would add valuable information to our research.

There is limited but growing evidence showing that the changes in biochemical composition in primary producers can be transferred to secondary and tertiary producers, and thereby potentially affect seafood quality and other marine ecosystem services (Jin et al. 2015; Hurd et al. 2018; Riebesell et al. 2018; Sswat et al. 2018). For instance, ocean acidification increased the accumulation of iodide in the brown alga *Saccharina japonica*, and consequently increased the levels of iodine in abalone feeding on them, thereby influence the seafood quality (Xu et al. 2019). Here we provide further evidence that the metabolite profile changes in a primary producer (diatom) would transfer via the food chain to alter the metabolite profiles in a secondary producer (clam). By integrating primary and secondary producer multi-omics data, we then elucidated the mechanisms underlying this food chain transfer, and found that the altered terpenoid backbone biosynthesis in the methylome and transcriptome led to the observed decrease of pyruvate and upregulation of certain pathways (e.g., phenylalanine metabolism) in the metabolome of primary producer, and these changes in metabolomic profile were then transferred to the secondary producer, resulting in the changes in abundance of some metabolites, such as decreases in pyruvate and increases in 2-hydroxylamino-4,6-dinitrotoluene. Although most Earth system models of the ecological consequences of global change do not consider food chain effects (Bonan and Doney 2018; Tagliabue 2023), the findings in the present study can be integrated into models and improve projections of marine ecosystem services and functions for the coming decades. Furthermore, the recently developed emergent models can also use omics data (e.g., genomics, transcriptomics) to observe biogeochemical outcomes (Follows et al. 2007; Mock et al. 2016; Strzepek et al. 2022), for example, to predict the assembly of communities based on functional repertoire (Coles et al. 2017). Taken together, our study suggests that the integration of multi-omics data across trophic levels, from primary producers to secondary producers, may provide more accurate projections of marine ecosystem services and functions over the next century.

Data availability statement

All data used to evaluate the conclusions in the paper are present in the paper and/or the Supplementary Information. Sequencing data are provided at the NCBI (SRA) database under the study accession code PRJNA824313.

References

Akalin, A., M. Kormaksson, S. Li, F. E. Garrett-Bakelman, M. E. Figueroa, A. Melnick, and C. E. Mason. 2012. methylKit: A comprehensive R package for the analysis of genome-wide DNA methylation profiles. Genome Biol. **13**: 1–9.

Arakawa, T., and S. Timasheff. 1985. The stabilization of proteins by osmolytes. Biophys. J. **47**: 411–414.

Bajguz, A. 2009. Brassinosteroid enhanced the level of abscisic acid in *Chlorella vulgaris* subjected to short-term heat stress. J. Plant Physiol. **166**: 882–886.

Bonan, G. B., and S. C. Doney. 2018. Climate, ecosystems, and planetary futures: The challenge to predict life in earth system models. Science **359**: eaam8328.

Bowler, C., and others. 2008. The *Phaeodactylum* genome reveals the evolutionary history of diatom genomes. Nature **456**: 239–244.

Boyd, P. W., and others. 2013. Marine phytoplankton temperature versus growth responses from polar to tropical waters-outcome of a scientific community-wide study. PLoS One **8**: e63091.

Chen, H., X. Gu, Q. Zeng, Z. Mao, and C. J. Martyniuk. 2021. Characterization of the GABAergic system in Asian *clam Corbicula fluminea*: Phylogenetic analysis, tissue distribution, and response to the aquatic contaminant carbamazepine. Comp. Biochem. Physiol. C Toxicol. Pharmacol. **239**: 108896.

Chen, S., Y. Zhou, Y. Chen, and J. Gu. 2018. fastp: An ultra-fast all-in-one FASTQ preprocessor. Bioinformatics **34**: i884–i890.

Clark, T. D., G. D. Raby, D. G. Roche, S. A. Binning, B. Speers-Roesch, F. Jutfelt, and J. Sundin. 2020. Ocean acidification does not impair the behaviour of coral reef fishes. Nature **577**: 370–375.

Coles, V. J., and others. 2017. Ocean biogeochemistry modeled with emergent trait-based genomics. Science **358**: 1149–1154.

Collins, S., P. W. Boyd, and M. A. Doblin. 2020. Evolution, microbes, and changing ocean conditions. Ann. Rev. Mar. Sci. **12**: 181–208.

Dunn, W. B., and others. 2011. Procedures for large-scale metabolic profiling of serum and plasma using gas chromatography and liquid chromatography coupled to mass spectrometry. Nat. Protoc. **6**: 1060–1083.

Esabyoglou, T., and G. Rimbach. 2017. Canthaxanthin: From molecule to function. Mol. Nutr. Food Res. **61**: 16000469.

Follows, M. J., S. Dutkiewicz, S. Grant, and S. W. Chisholm. 2007. Emergent biogeography of microbial communities in a model ocean. Science **315**: 1843–1846.

Gleason, L. U., L. P. Miller, J. R. Winnikoff, G. N. Somero, P. H. Yancey, D. Bratz, and W. W. Dowd. 2017. Thermal history and gape of individual *Mytilus californianus* correlate with oxidative damage and thermoprotective osmolytes. J. Exp. Biol. **220**: 4292–4304.

Guillard, R. R., and J. H. Ryther. 1962. Studies of marine planktonic diatoms: I. *Cyclotella nana* Hustedt, and *Detonula confervacea* (Cleve) Gran. Can. J. Microbiol. **8**: 229–239.

Hartung, W. 2010. The evolution of abscisic acid (ABA) and ABA function in lower plants, fungi and lichen. Funct. Plant Biol. **37**: 806–812.

Holm, H. C., H. F. Fredricks, S. M. Bent, D. P. Lowenstein, J. E. Ossolinski, K. W. Becker, W. M. Johnson, K. Schrage, and B. A. S. van Mooy. 2022. Global ocean lipidomes show a universal relationship between temperature and lipid unsaturation. Science **376**: 1487–1491.

Huang, T., and others. 2024. Multi-omics analysis reveals the associations between altered gut microbiota, metabolites, and cytokines during pregnancy. mSystems. **9**: e01252-23.

Hurd, C. L., A. Lenton, B. Tilbrook, and P. W. Boyd. 2018. Current understanding and challenges for oceans in a higher-CO_2 world. Nat. Clim. Change **8**: 686–694.

IPCC. 2021. Climate change 2021. *In* V. Masson-Delmotte and others [eds.], The physical science basis. Contribution of Working Group I to the Sixth Assessment Report of the Intergovernmental Panel on Climate Change. Cambridge University Press.

Jessen, K. R., R. Mirsky, M. E. Dennison, and G. Burnstock. 1979. GABA may be a neurotransmitter in the vertebrate peripheral nervous system. Nature **281**: 71–74.

Jiang, H., and K. Gao. 2004. Effects of lowering temperature during culture on the production of polyunsaturated fatty acids in the marine diatom *Phaeodactylum tricornutum* (Bacillariophyceae). J. Phycol. **40**: 651–654.

Jin, P., T. Wang, N. Liu, S. Dupont, J. Beardall, P. W. Boyd, U. Riebesell, and K. Gao. 2015. Ocean acidification increases the accumulation of toxic phenolic compounds across trophic levels. Nat. Commun. **6**: 8714.

Jin, P., G. Gonzàlez, and S. Agustí. 2020. Long-term exposure to increasing temperature can offset predicted losses in marine food quality (fatty acids) caused by ocean warming. Evol. Appl. **13**: 2497–2506.

Jin, P., and others. 2022*a*. A reduction in metabolism explains the tradeoffs associated with the long-term adaptation of phytoplankton to high CO_2 concentrations. New Phytol. **233**: 2155–2167.

Jin, P., and others. 2022*b*. Increased genetic diversity loss and genetic differentiation in a model marine diatom adapted to ocean warming compared to high CO_2. ISME J. **16**: 2587–2598.

Kim, D., B. Langmead, and S. L. Salzberg. 2015. HISAT: A fast spliced aligner with low memory requirements. Nat. Methods **12**: 357–360.

Kumar, B., C. Kaur, A. Pareek, S. K. Sopory, and S. L. Singla-Pareek. 2021. Tracing the evolution of plant glyoxalase III enzymes for structural and functional divergence. Antioxidants. **10**: 648.

Langmead, B., and S. L. Salzberg. 2012. Fast gapped-read alignment with Bowtie 2. Nat. Methods **9**: 357–359.

Leles, S. G., and N. M. Levine. 2023. Mechanistic constraints on the trade-off between photosynthesis and respiration in response to warming. Sci. Adv. **9**: eadh8043.

Lister, R., and others. 2009. Human DNA methylomes at base resolution show widespread epigenomic differences. Nature **462**: 315–322.

Listmann, L., M. LeRoch, L. Schlüter, M. K. Thomas, and T. B. H. Reusch. 2016. Swift thermal reaction norm evolution in a key marine phytoplankton species. Evol. Appl. **9**: 1156–1164.

Liu, H., J. X. Zhu, H. L. Sun, J. G. Fang, R. C. Gao, and S. L. Dong. 2006. The clam, Xishi tongue *Coelomactra ahtiquata* (Spengler), a promising new candidate for aquaculture in China. Aquaculture **255**: 402–409.

Mock, T., S. J. Daines, R. Geider, S. Collins, M. Metodiev, A. J. Millar, V. Moulton, and T. M. Lenton. 2016. Bridging the gap between omics and earth system science to better understand how environmental change impacts marine microbes. Glob. Chang. Biol. **22**: 61–75.

Moreno, H. D., and others. 2023. Higher temperature, increased CO_2, and changing nutrient ratios alter the carbon metabolism and induce oxidative stress in a cosmopolitan diatom. Limnol. Oceanogr. **69**: 121–139. doi:10.1002/lno.12463

Nagelkerken, I., S. Goldenberg, C. Ferreira, H. Ullah, and S. Connell. 2020. Trophic pyramids reorganize when food web architecture fails to adjust to ocean change. Science **369**: 829–832.

Nilsson, G., and others. 2012. Near-future carbon dioxide levels alter fish behaviour by interfering with neurotransmitter function. Nat. Clim. Change. **2**: 201–204.

Peng, C., X. Zhao, S. Liu, W. Shi, Y. Han, C. Guo, X. Peng, X. Chai, and G. Liu. 2017. Ocean acidification alters the burrowing behaviour, Ca^{2+}/Mg^{2+}-ATPase activity, metabolism, and gene expression of a bivalve species, *Sinonovacula constricta*. Mar. Ecol. Prog. Ser. **575**: 107–117.

Pérez, E. B., I. C. Pina, and L. P. Rodríguez. 2008. Kinetic model for growth of *Phaeodactylum tricornutum* in intensive culture photobioreactor. Biochem. Eng. J. **40**: 520–525.

Reusch, T. B., and P. W. Boyd. 2013. Experimental evolution meets marine phytoplankton. Evolution **67**: 1849–1859.

Riebesell, U., and others. 2018. Toxic algal bloom induced by ocean acidification disrupts the pelagic food web. Nat. Clim. Change **8**: 1082–1086.

Roede, J. R., K. Uppal, Y. Park, V. Tran, and D. P. Jones. 2014. Transcriptome-metabolome wide association study (TMWAS) of maneb and paraquat neurotoxicity reveals network level interactions in toxicologic mechanism. Toxicol. Rep. **1**: 435–444.

Rossoll, D., R. Bermúdez, H. Hauss, K. G. Schulz, U. Riebesell, U. Sommer, and M. Winder. 2012. Ocean acidification-induced food quality deterioration constrains trophic transfer. PLoS One **7**: e34737.

Sabir, J. S., and others. 2018. Phylogenetic analysis and a review of the history of the accidental phytoplankter, *Phaeodactylum tricornutum* Bohlin (Bacillariophyta). PLoS One **13**: e0196744.

Saradhi, P. P., I. Suzuki, A. Katoh, A. Sakamoto, P. Sharmila, D. J. Shi, and N. Murata. 2000. Protection against the photo-induced inactivation of the photosystem II complex by abscisic acid. Plant Cell Environ. **23**: 711–718.

Schlüter, L., K. T. Lohbeck, M. A. Gutowska, J. P. Gröger, U. Riebesell, and T. B. H. Reusch. 2014. Adaptation of a globally important coccolithophore to ocean warming and acidification. Nat. Clim. Change. **4**: 1024–1030.

Singh, D., R. Carlson, D. Fell, and M. Poolman. 2015. Modelling metabolism of the diatom *Phaeodactylum tricornutum*. Biochem. Soc. Trans. **43**: 1182–1186.

Sswat, M., M. H. Stiasny, J. Taucher, M. Algueró-Muñiz, L. T. Bach, F. Jutfelt, U. Riebesell, and C. Clemmesen. 2018. Food web changes under ocean acidification promote herring larvae survival. Nat. Ecol. Evol. **2**: 836–840.

Stickle, W. B., M. Lindeberg, and S. D. Rice. 2010. Seasonal freezing adaptations of the mid-intertidal *gastropod Nucella lima* from southeast Alaska. J. Exp. Mar. Biol. Ecol. **395**: 106–111.

Strzepek, R. F., B. L. Nunn, L. T. Bach, J. A. Berges, E. B. Young, and P. W. Boyd. 2022. The ongoing need for rates: Can physiology and omics come together to co-design the measurements needed to understand complex ocean biogeochemistry? J. Plankton Res. **44**: 485–495.

Szabados, L., and A. Savouré. 2010. Proline: a multifunctional amino acid. Trends Plant Sci. **15**: 89–97.

Tagliabue, A. 2023. "Oceans are hugely complex": Modelling marine microbes is key to climate forecasts. Nature **623**: 250–252.

Taucher, J., L. T. Bach, A. F. Prowe, T. Boxhammer, K. Kvale, and U. Riebesell. 2022. Enhanced silica export in a future ocean triggers global diatom decline. Nature **605**: 696–700.

Wan, J., and others. 2023. DNA methylation and gene transcription act cooperatively in driving the adaptation of a marine diatom to global change. J. Exp. Bot. **74**: 4259–4276.

Wang, C., L. N. Segal, J. Hu, B. Zhou, R. B. Hayes, J. Ahn, and H. Li. 2022. Microbial risk score for capturing microbial characteristics, integrating multi-omics data, and predicting disease risk. Microbiome. **10**: 121.

Worley, B., and R. Powers. 2013. Multivariate analysis in metabolomics. Curr. Metabolomics **1**: 92–107.

Xi, Y., and W. Li. 2009. BSMAP: Whole genome bisulfite sequence MAPping program. BMC Bioinformatics **10**: 1–9.

Xu, D., and others. 2019. Ocean acidification increases iodine accumulation in kelp-based coastal food webs. Glob. Chang. Biol. **25**: 629–639.

Yan, Z., and others. 2022. Multi-omics analyses of airway host-microbe interactions in chronic obstructive pulmonary disease identify potential therapeutic interventions. Nat. Microbiol. **7**: 1361–1375.

Yancey, P. H. 2005. Organic osmolytes as compatible, metabolic and counteracting cytoprotectants in high osmolarity and other stresses. J. Exp. Biol. **208**: 2819–2830.

Zeng, X., and others. 2020. Light alters the responses of two marine diatoms to increased warming. Mar. Environ. Res. **154**: 104871.

ACKNOWLEDGMENTS

We thank Guangzhou Genedenovo Biotechnology Co., Ltd for assisting in sequencing and/or bioinformatics analysis. The University of Dundee is a Scottish registered charity, no. 051096. This study was supported by the National Natural Science Foundation of China (nos. 41806141, 42076109, and 42076206), Natural Science Foundation of Guangdong Province (2023A1515030286, 2020A1515011073), Guangzhou Municipal Science and Technology Bureau (202201020151), the fund of Guangdong Provincial Key Laboratory of Fishery Ecology and Environment (FEEL-2022-2), Earth Critical Zone and Eco-geochemistry (PT252022024), and GuangzhouU-HKUST Joint Research Fund (202005).

Conflict of Interest

None declared.

Submitted 20 February 2024
Revised 21 April 2024
Accepted 27 May 2024

Associate editor: Bingzhang Chen